Purdue University
Purdue e-Pubs

International Refrigeration and Air Conditioning Conference

School of Mechanical Engineering

2014

Self-healing, Slippery Surfaces for HVAC&R Systems

Rong Yu
University of Illinois at Urbana-Champaign, United States of America, rongyu2@illinois.edu

Anthony M. Jacobi
University of Illinois at Urbana-Champaign, United States of America, a-jacobi@illinois.edu

Follow this and additional works at: http://docs.lib.purdue.edu/iracc

Yu, Rong and Jacobi, Anthony M., "Self-healing, Slippery Surfaces for HVAC&R Systems" (2014). *International Refrigeration and Air Conditioning Conference.* Paper 1378.
http://docs.lib.purdue.edu/iracc/1378

This document has been made available through Purdue e-Pubs, a service of the Purdue University Libraries. Please contact epubs@purdue.edu for additional information.
Complete proceedings may be acquired in print and on CD-ROM directly from the Ray W. Herrick Laboratories at https://engineering.purdue.edu/Herrick/Events/orderlit.html

Self-healing, Slippery Surfaces for HVAC&R Systems

Rong Yu[1]*, and Anthony M. Jacobi[2]

[1]University of Illinois at Urbana-Champaign, Dept. of Mechanical Science & Engineering,
Urbana, Illinois 61801, USA
rongyu2@illinois.edu

[2]University of Illinois at Urbana-Champaign, Dept. of Mechanical Science & Engineering,
Urbana, Illinois 61801, USA
a-jacobi@illinois.edu

* Corresponding Author

ABSTRACT

Enhancing water shedding behavior on aluminum surfaces is important in the design of energy-efficient heat exchangers. In this work, a method for fabricating oil-infused aluminum surfaces for HVAC&R systems is described for the purpose of exploiting the slippery nature of such surfaces, thereby improving the overall surface wettability. A microstructured, porous aluminum fin stocks with heterogeneous hydrophobic coating are infused with a secondary liquid acting as a lubricant that enhances slippery, liquid repellant and self-healing behavior. The objective of this work is to study the feasibility of using these surfaces to more effectively manage condensate/frost formation on heat exchangers. The effects of the underlying oil-infused microstructure and hydrophobic coating on the behavior of droplets are studied. Although the slippery surfaces are observed to decrease the contact angle of droplets, they promote mobility by reducing the interfacial energy and friction force. From preliminary experiments, critical inclination angles of small droplets (volume $\leq$30 μl) are reduced by more than 40° compared to baseline surfaces. Moreover, slippery surfaces delay the frost formation, and have only one fourth of the baseline water retention after self-defrosting. Therefore, such properties provide potential for improving the water drainage behavior for HVAC&R systems.

1. INTRODUCTION

Water retention on the air-side surface of metallic heat exchangers poses economic and safety issues (i.e. lower efficiency, enhancement of pressure drop and health hazard due to the growth of bacteria). Prior works have focused on the liquid repellent micro-structured surfaces (Sommers and Jacobi 2006, Rahman, *et al.* 2012, and Yu, *et al.* 2013). However, these surfaces have limited oleophobicity (Tuteja, *et al.* 2008), potential to be damaged (Quere 2008), or high manufacturing cost. In order to address some of these drawbacks, the development of an omniphobic, self-healing surface has been pursued. Inspired by the super-slippery surfaces of *Nepenthes* (Pitcher Plants), such surfaces were made possible by locking a liquid solution into the micro- or nano- structured surface (Bohn and Federle 2004). Synthetic surfaces mimicking this slippery, liquid-repellant, self-healing behavior have been recently reported (Wong *et al.* 2011, Kim *et al.* 2012, Xiao *et al.* 2013 and Rykaczewski *et al.* 2013). However, the potential applications of such surfaces on HVAC&R systems and their effects on thermal-hydraulic performance have not been considered in earlier works.

In the current work, a method for fabricating slippery aluminum surfaces for mass production is discussed. Using the specimens thus developed, experiments are performed for evaluating the suitability of such surfaces for managing water in HVAC&R applications. Various methods are employed to assess the behavior of water on these novel surfaces, including static contact angle measurements, sliding angle measurements, and condensation/ frosting experiments.

2. EXPERIMENTAL METHOD

2.1 Fabrication of Slippery Surface

The 2.54cm x 2.54 cm (1" x 1") aluminum substrate was made of Al alloy 1100 (99.9% pure Al). In order to remove all surface contaminants, the aluminum samples were first cleaned with acetone, followed by an ultrasonic water bath, and then were dried with nitrogen gas. Afterwards, the samples were anodized using high purity platinum as the cathode under a constant voltage of 10 V in an aqueous solution containing sulfuric acid (20 w/o) at room temperature for 15 min as shown in Fig. 1. The area ratio of the two electrodes was 1:1 and the distance between them was 3 cm. The specimen was anodized to form a porous alumina outer layer microstructure with an average thickness of 8.6±3.1μm (see Fig. 2). These microstructures were created for the purpose of locking the secondary liquid into the surface.

After the anodization, the cleaned specimens were coated by heptadecafluoro tetra hydrodecyl-trichlorosilane (FDTS) using molecular vapor deposition (MVD) (Applied Microstructures). The MVD process deposited a monolayer hydrophobic coating on the surface which altered surface wettability by changing surface free energy. From the X-ray photoelectron spectroscopy (XPS) image analysis of anodized aluminum, it was found that the substrate had a composition of more than 95% aluminum oxide; the rest was aluminum sulfate (see Fig. 3a). The XPS images showed Si and Al peaks from the underlying substrate; however, no Cl peak was observed, indicating the small thickness of FDTS coating (see Fig. 3b). Perfluoropolyether (PFPE) was chosen as the secondary liquid, since PFPE has low volatility, surface tension (σ=21 mN m^{-1}) and is immiscible with both aqueous and hydrocarbon phases (Ma *et al.*, 2013). The secondary liquid was infused into surface by capillary force.

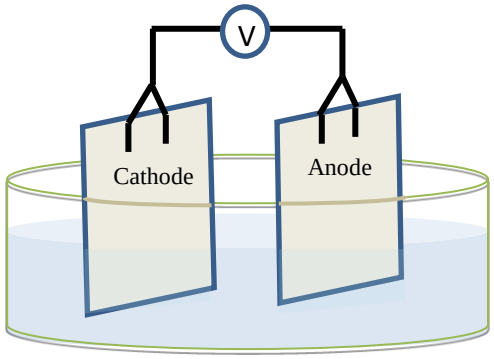

Figure 1: Schematic of anodization apparatus

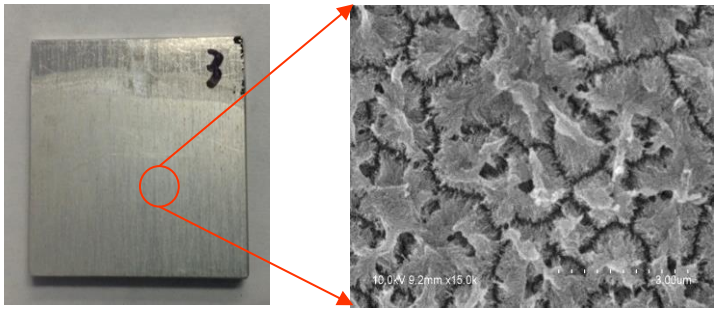

Figure 2: Photograph of a sample specimen with SEM image showing underlying microstructure

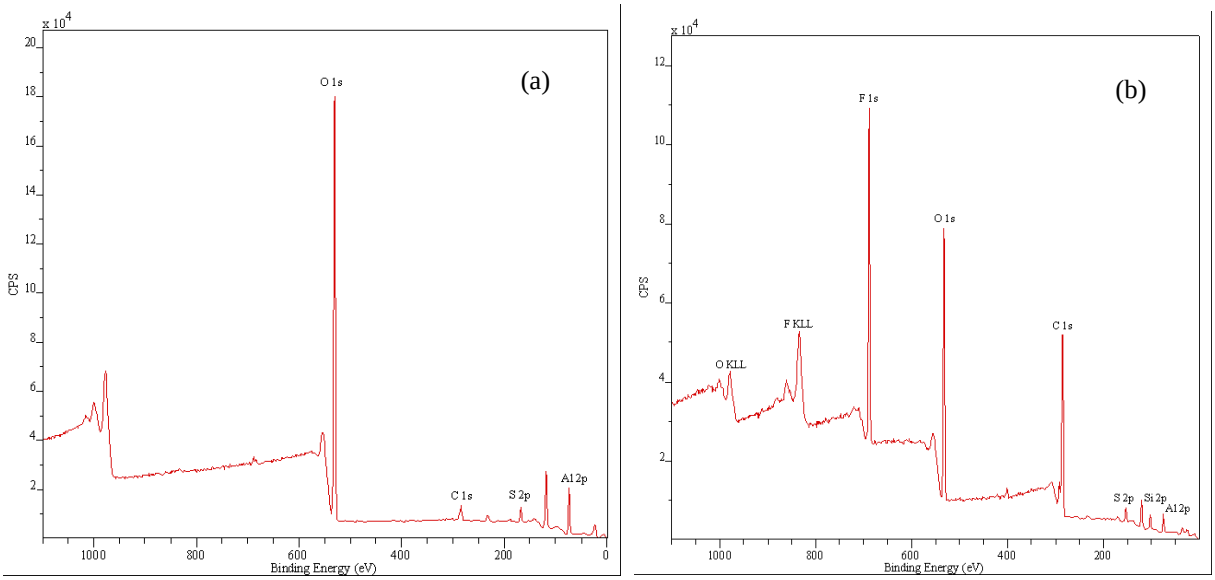

Figure 3: XPS results of anodized aluminum rough surface (a) and hydrophobic rough surface (b)

2.2 Static Contact Angle and Critical Inclination Angle Measurements

Contact angle and sliding angle are important parameters used in characterizing and assessing the overall wettability of a surface. Contact angle measurements with an accuracy of ±0.1° were conducted using a CAM200 (KSV Instruments) optical goniometer in a class-100 cleanroom facility. Water droplets (5 µl) were injected on the surface using an automated dispenser. A high speed camera was used to capture the drop shape throughout the entire process for images analysis. The Young-Laplace equation was used for curve fitting.

For critical inclination angle measurements, a droplet was placed on horizontal test sample using a precision micro-pump. The volume of the droplet was from 10µl to 70µl. The sample holder was then slowly tilted using a threaded rod under the holder until imminent droplet motion was detected. The process was recorded using a high speed camera (Phantom v640).

2.3 Condensation/Frosting Experiments

The condensation and frosting experiments were conducted in a thermally controlled chamber (see Fig. 4). The chamber was made of Plexiglas and has dimensions of 30×30×22 cm^3. The chamber was fixed on a stable frame. A humidifier was used to provide cold mist inside the chamber. Two hygrometers (Omega logger, accuracy: ±2%) were attached to monitor the relative humidity inside the chamber. A vortex tube cooler (EXAIR corporation, Model-3225) provided two streams of compressed air for the experiments. The cold air was injected into chamber. A slotted valve regulated the flow rate of the hot stream, and was used to adjust the temperature and flow rate of the cold air. The pressure of compressed air was about 60 kPa. The air velocity was measured at different points inside the chamber using a hot wire anemometer (VelociCalc®, uncertainty ±0.01 m/s). The sample was mounted on a Peltier cold plate by copper conductive tape to ensure better thermal contact. Thermocouples (uncertainty of ±0.2 ˚C) were used to measurement temperatures of the sample, inside and outside chamber. Four thermocouples were inserted into holes made at the side of the sample. In order to minimize thermal resistance, the air gaps between holes and thermocouples were filled with thermally conductive paste (Omegatherm®, 2.31 W/m-K). The temperature data were recorded and analyzed using Labview Software (National Instruments). The images of condensation/frosting process were obtained using a high speed camera (Phantom v640).

The specimen was kept inside the chamber in the vertical direction. After a certain freezing time, the specimen was taken out of the chamber and was defrosted under natural convection. The frost drainage was collected on dry filter papers until the plate temperature rose by 5 ˚C. The dry and wet filter papers were weighted on a balance (Mettler, ±0.0001g). The difference in mass between the wet and dry filter papers yielded the mass of frost drainage. The water retention ratio, calculated according to Eq. (1), was used for characterizing the surface performance of various samples.

$$Ratio = \frac{Mass_{waterretention}}{Mass_{frost}} \quad (1)$$

A smaller water retention ratio implies better surface performance, i.e. less pressure drop, and potential enhancement of heat transfer.

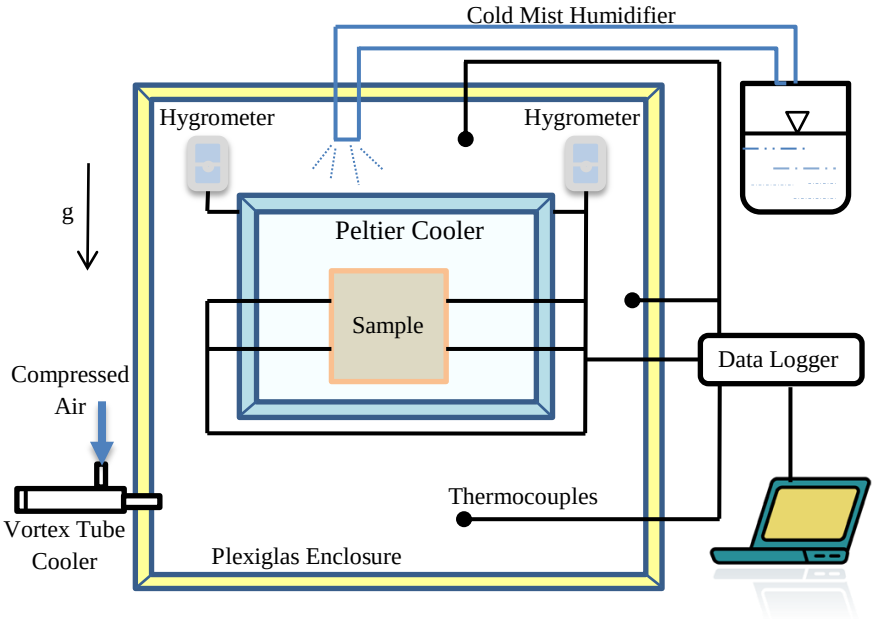

Figure 4: Schematic of the apparatus for condensation/frosting experiments

3. EXPERIMENTAL RESULTS AND DISCUSSION

3.1 Static Contact Angle and Critical Inclination Angle Results

Contact angle experiments were conducted on the following aluminum surfaces: baseline surface with and without coating, anodized surface with and without coating, and two liquid infused surfaces. The results are summarized in Table 1.

Table 1: Water droplet contact angle data

Surfaces	Contact angle, °
Bare Aluminum (baseline)	90.6 ±1.2
Bare Al + MVD (phobic flat)	113.5±1.5
Anodized Aluminum (rough)	≈ 0
Anodized Al +PFPE	≈ 0
Anodized Al+ MVD (phobic rough)	130.2±5.9
Anodized Al + MVD +PFPE (slippery)	105.0±3.5

Compared to the baseline, the FDTS coated surface showed increased hydrophobicity with a larger contact angle. Because the density of water is only one third that of PFPE, the water droplet floats on the oil. The depth of water droplet immersed in the oil calculated from Young's Equation is much larger than the oil layer infused into porous surfaces. This implies that the water droplet sits on the surface and has a direct contact with the substrate. Therefore, the FDTS coating directly affects the contact angle of the droplet with/without PFPE. Microstructures made by the anodization process increased the surface roughness. This roughness made hydrophilic surfaces more hydrophilic and hydrophobic surfaces more hydrophobic as the Wenzel (1936) and the Cassie-Baxter (1944) models suggest.

Results from the critical inclination angle measurements for various surfaces are presented in Fig. 5. The surfaces without any oil infused have the roughness which increases the surface hydrophobicity, but also have many pins which hinder the drainage of the water droplet. Therefore, the flat hydrophobic surface had a similar sliding angle to that of a phobic rough surface. For surfaces with oil infused, the oil layer effectively reduces the number of pins on the surfaces, thereby lowering the sliding angle. Moreover, the oil/water interface has less surface tension compared to the solid/water interface. The enhancement was also observed for the surface with oil depletion (the amount of oil was 0.003g). In addition, sliding angle data for oil infused surfaces have less dependent on the volume of water droplet compared to surfaces without oil. Overall, the PFPE infused in the surface reduced the contact angle of the droplet, however, the mobility of droplet was improved by PFPE.

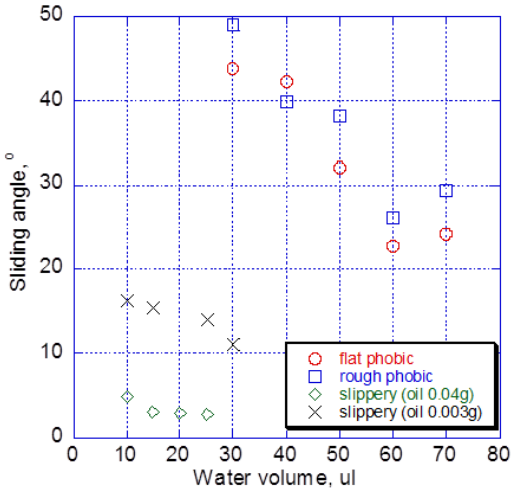

Figure 5: Critical inclination angle measurements for various surfaces

3.2 Condensation/Frosting Experiments

The baseline, phobic rough and slippery surfaces were placed on the cold plate. The duration of each frosting cycle was about three hours. The chamber temperature and relative humidity were maintained at about 6-8 ˚C and 70%-80% RH, respectively. The cold plate was kept at three different temperatures, since plate temperature may affect the frost density and defrost rate. The defrosted occurred due to natural convection at room temperature (around 20-21 °C) and 50%-55% RH.

During the frosting cycle, the temperature of the specimen on the cold plate decreased gradually until a steady state condition was achieved. In addition, the temperature in the chamber was above freezing point. Therefore, water condensed on the surface first, and then froze. When the temperature of specimen was below the dew point, it is expected that the water started to condense on the oil/air interface rather than oil/solid interface. The change in system Gibbs free energies of each condition is calculated under experimental conditions using Eqns. 2 and 3, respectively.

$$\Delta G_{oil-air} = m\cdot(g_w - g_v) - V\cdot(P_w - P_v) + 4\pi r^2 f(\theta)\sigma_{wv} < 0 \quad (2)$$

$$\Delta G_{oil-solid} = m\cdot(g_{after} - g_{before}) + V\cdot(P_o - P_w) + A_{ow}\cdot\sigma_{ow} - A_{sw}\cdot(\sigma_{so} - \sigma_{ws}) > 0 \quad (3)$$

Where $f(\theta) = \frac{2 - 3\cos\theta + \cos^3\theta}{4}$, $A_{ow} = 2\pi r^2\cdot(1-\cos\theta)$, and $A_{sw} = \pi r^2\cdot(1-\cos^2\theta)$.

The system free energy decreases when droplets nucleate on the oil/air interface, but increases when nucleation occurs on the oil-solid interface. Since the Gibbs free energy is a minimum at a stable equilibrium, droplets forming on the oil-air interface are expected. Before the water froze, condensed water was covered by an oil monolayer because of the positive spreading coefficient. (Note: The spreading coefficient is defined as

$Sp_{ow} = \sigma_{wv} - \sigma_{ov} - \sigma_{ow}$). When the spreading coefficient is positive, the oil will spontaneously spread on the surface of water (Carey, 2008). Small droplets grew bigger and drained due to gravity. Some small droplets made contact, maintained the water-oil interface, and eventually coalesced into a big droplet (see two circle markers in Figure 6). In addition, it was observed that the oil-infused surface delayed freezing.

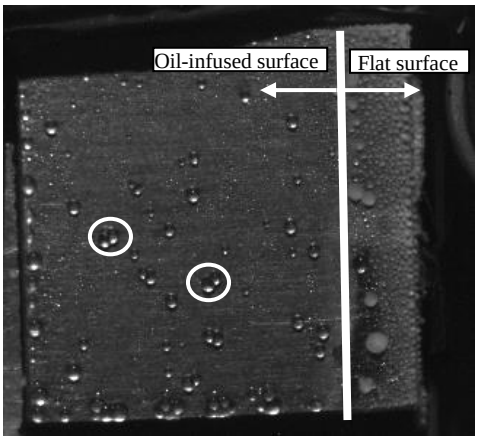

Figure 6: A photograph of the oil-infused surface during frosting/ defrosting experiment

The water retention ratios of various specimens at three plate temperatures are shown in Fig. 7. The slippery surface retained less water and hence had a lower water retention ratio (~ 1%) compared to other surfaces (~ 4-6%). The water retention ratio of the slippery surface decreased by three fourths of baseline. Although the hydrophobic rough surface has larger contact angle (~ 130˚) than that of the oil-infused surface (~ 105˚), existence of oil on the surface reduced the friction and promoted the water drainage behavior. Surfaces except the slippery one showed similar behavior. The water retention ratio was unaffected by the temperature of the cold plate.

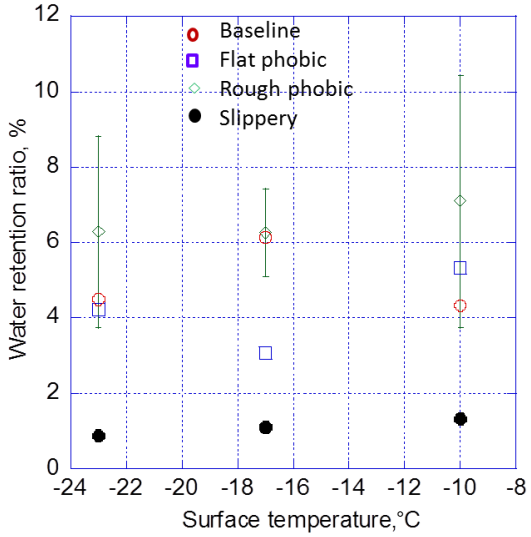

Figure 7: The water retention ratio for various surfaces at different plate temperatures

For the refrosting/defrosting tests, the samples were subject to previously mentioned frosting and defrosting cycles. The first frosting/defrosting cycle was not considered, therefore some water was retained on the surface. The sample was again put back to the controlled chamber for another frosting/defrosting cycle. The mass of water removed and retained were determined after the second cycle. The comparison of water retention ratios of the first and second cycle is shown in Fig. 8. The water retention on the surface increases with frosting/defrosting cycles. The main reason for such deteriorating water retention behavior is due to the depletion of oil during experiments. In addition, the water retention ratio of frosting/defrosting test is almost same as refrosting/defrosting test. This implies that the

water retention from the previous cycle did not affect much on the water retention ratio of the following cycle. A possible reason for such behavior might be the retained water drained before freezing.

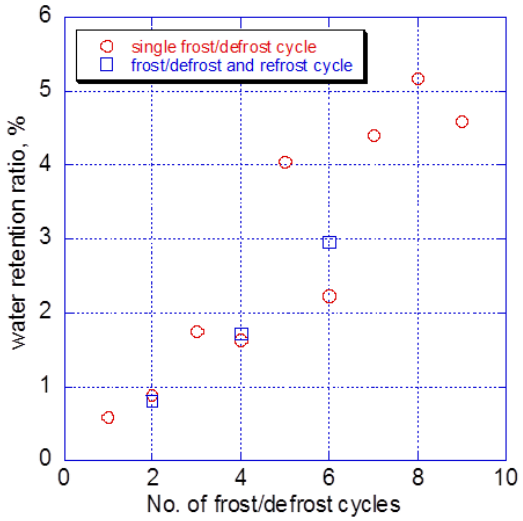

Figure 8: The water retention ratio on slippery surface under different cycles

4. CONCLUSIONS

The present study reports a novel surface treatment for heat transfer surfaces in HVAC&R systems, where condensate, frost, or frost-melt management is important. The slippery surface provides more liquid/liquid interface rather than solid/liquid interface, resulting in a significant increase in droplet mobility, which may make this kind of surface valuable in application. On the basis of this work, the following conclusions are drawn:

- The PFPE infused on the surface reduced the contact angle of water; however, the mobility of droplet was improved by PFPE.
- The slippery surface had at least three times less water retention ratio than other surfaces.
- A delay in frost formation was observed on the slippery surface.
- The water retention on the slippery surface did not affect water retention ratio of refrost/defrost cycle.
- Oil depletion was observed during condensation/frosting experiments. Possible techniques for minimizing the oil depletion need to be explored.

NOMENCLATURE

A	Area	(m^2)
g	Specific Gibbs function	(J/kg)
G	Gibbs function	(J)
m	Mass of nuclei	(kg)
P	Pressure	(Pa)
r	Radius of nuclei	(m)
v	Specific volume	(m^3/kg)
V	Volume of nuclei	(m^3)

Greek symbols

σ	interfacial tension	(N/m)
Θ	contact angle	(°)

Subscript

o	PFPE oil
s	substrate

v vapor
w water

REFERENCES

Bohn, H.F., Federle, W., 2004, Insect aquaplaning: *Nepenthes* pitcher plants capture prey with the peristome, a fully wettable water-lubricated anisotropic surface, *Proceedings of the National Academy of Sciences of the USA*, vol. 101: p. 14138-14143.

Carey, V.P., 2008, *Liquid-Vapor Phase-Change Phenomena*, Taylor &Francis Group, LLC, New York, 742p.

Cassie, A.B.D., Baxter, S., 1944, Wettability of porous surfaces, *Trans. Faraday Soc*., vol. 40: p. 546-551.

Kim, P., Wong, T.-S., Alvarenga, J., Kreder, M.J., Adorno-Martinez, W.E., Aizenberg, J., 2012, Liquid-infused nanostructured surfaces with extreme anti-ice and anti-frost performance, *ACS Nano*, vol. 6: p.6569-6577.

Ma, W., Higaki, Y., Otsuka, H., Takahara, A., 2013, Perfluoropolyether-infused nano-texture: a versatile approach to omniphobic coatings with low hysteresis and high transparency, *The Royal Society of Chemistry*, vol. 49, no. 6: p. 597-599.

Quere, D., 2008, Wetting and roughness, *Annual Review of Materials Research*, vol. 38: p. 71-99.

Rahman, M.A., Jacobi, A.M., 2012, Wetting behavior and drainage of water droplets on microgrooved brass surfaces, *Langmuir*, vol. 28, no. 37: p. 13441-13451.

Rykaczewski, K., Anand, S., Subramanyam, S.B., Varanasi, K.K., 2013, Mechanism of frost formation on lubricant-impregnated surfaces, *Langmuir*, vol. 29: p. 5230-5238.

Sommers, A.D., Jacobi, A.M., 2006, Creating micro-scale surface topology to achieve anisotropic wettability on an aluminum surface, *Journal of Micromechanics and Microengineering*, vol. 16, no.8: p.1571-1578.

Tuteja, A., Choi, W., Mabry, J.M., McKinley, G.H., Cohen, R.E., 2008, Robust omniphobic surfaces, *Proceedings of the National Academy of Sciences of the USA*, vol. 105, no. 47: p. 18200-18205.

Wenzel, R., 1936, Resistance of solid surfaces to wetting by water, *Ind. Eng. Chem*., vol. 28: p. 988-994.

Wong, T.-S., Kang, S.H., Tang, S.K.Y., Smythe, E.J., Hatton, B.D., Grinthal, A., Aizenberg, J., 2011, Bioinspired self-repairing slippery surfaces with pressure-stable omniphobicity, *Nature*, vol. 477: p. 443-447.

Xiao, R., Miljkovic, N., Enright, R., Wang, E.N., 2013, Immersion condensation on oil-infused heterogeneous surfaces for enhanced heat transfer, *Scientific Reports*, vol. 3: 1988.

Yu, R., Sommers, A.D., Okamoto, N.C., 2013, Effect of a micro-grooved fin surface design on the air-side thermal-hydraulic performance of a plain fin-and-tube heat exchanger, *Int. Journal of Refrigeration*, vol. 36, no. 3: p. 1078-1089.

ACKNOWLEDGEMENT

The authors would like to express gratitude for financial support from Air Conditioning and Refrigeration Center (ACRC) at the University of Illinois at Urbana-Champaign.